



**White paper**

# *syngo.via* Database Comparison in MI Neurology

Rachid Fahmi, PhD  
Guenther Platsch, MD

[siemens-healthineers.com/mi](https://www.siemens-healthineers.com/mi)

# Table of Contents

<b>Introduction</b>	<b>3</b>
<b>Interpretation of database comparison statistics</b>	<b>4</b>
Voxel-based statistics	4
Region of interest-based statistics	9
<b>Processing prior to analysis</b>	<b>10</b>
Database selection	10
Rigid registration of anatomical data	11
Alignment of subject images to database	11
Smoothing	12
Intensity normalization	12
<b>Database construction</b>	<b>13</b>
Individual database details: FDG-PET	13
Individual database details: florbetapir-PET	15
Individual database details: florbetaben-PET	16
Individual database details: ECD-SPECT	16
Individual database details: HMPAO-SPECT	18
User-created databases	18
<b>Spatial normalization for database alignment</b>	<b>19</b>
FDG-PET	19
Beta amyloid-PET	19
ECD- and HMPAO-SPECT	19
Manual adjustment	20
CT-based affine alignment	20
<b>Summary displays</b>	<b>21</b>
Standard stereotactic surface projection	21
Modified stereotactic surface projection	23
<b>Potential artifacts</b>	<b>24</b>
Abnormal subject brain structure	24
Registration artifacts	25
Intensity normalization issues	26
Abnormal area of uptake	27
Atrophy artifact for florbetapir-PET images	27
Marrow uptake artifact for amyloid PET images	28
<b>Conclusion</b>	<b>29</b>
<b>About the authors</b>	<b>29</b>
<b>Acknowledgment</b>	<b>29</b>
<b>References</b>	<b>30</b>

*syngo.PET Amyloid Plaque is intended for use only with approved amyloid radiopharmaceuticals in the country of use. Users should review the drug labeling for approved uses.*

# Introduction

Database Comparison is a software solution that enables the user to compare a brain PET or SPECT scan of a patient to a database of brain images of the same radiotracer composed of scans from confirmed normal individuals. Comparison to such a database is a commonly used technique in molecular imaging brain analysis and provides information that can be useful in the assessment of brain diseases. After a clinical visual assessment is made of the brain scan and a diagnosis is proposed<sup>1</sup>, Database Comparison can be used to confirm the first impression from the visual read by providing regional quantification of deviation from normal tracer uptake. Artifacts (e.g. due to patient motion or attenuation correction problems) should be recorded, because Database Comparison is not able to differentiate artifacts in the input data from real medical findings and will present them in the same way.

All findings of Database Comparison should be compared to the initial visual impressions: any discrepancies require further investigation such as direct comparison between the original data and the Database Comparison results (which will solve many issues), comparison to diagnostic MR or CT (e.g. large sulci, individual anatomical variations without disease value, malformations, infarctions, and tumors) as well as other clinical information. Any findings from the database comparison without correlation to the uptake images should be treated with great care. The “Potential Artifacts” section describes some of the more commonly seen artifacts and how to identify them.

The purpose of this white paper is to describe the tools provided by Database Comparison, as available in *syngo*®.via, for use with a typical analysis and to give technical details about the processing applied to data during the analysis. The “Interpretation of Database Comparison Statistics” section starts by using some clinical examples as motivation, providing references to later parts of the document for further details.

# Interpretation of database comparison statistics

The main purpose of the Database Comparison workflow is to calculate and display voxel-wise comparison statistics, highlighting areas of the subject dataset where tracer uptake is different from that in the normal population used to build the selected database. The “Processing Prior to Analysis” section provides the details of the processing required to get to the point where an analysis can be reliably performed, but once there, comparison to the database provides statistics in two forms:

1. Voxel-based statistics displayed as an image volume
2. Region of interest statistics

Both types of statistics are calculated by comparing the corresponding mean value estimated for the normal population to the value from the subject and dividing by the corresponding standard deviation of values estimated from the normal population as in Equation 1 below.

Equation 1: Calculation of statistics from estimated population mean and standard deviation and subject value.

$$\text{statistic} = \frac{(\text{patientValue} - \text{populationMean})}{\text{populationStandardDeviation}}$$

The statistic thus represents distance from the estimated population mean relative to the estimated population standard deviation (e.g. the number of standard deviations from the population mean, “#Std. Dev.”), which allows for differences in variation in the normal population in different regions of the brain.

## Voxel-based statistics

Voxel-based statistics in Database Comparison are shown using a standard color-table (LUT) across all tracers for both PET and SPECT images. A fixed range of intensities is used for any particular tracer, ensuring that particular colors in the image correspond to the same value of the underlying statistic for all datasets acquired with the same tracer and modality. Note, however, that a slightly different range is used for SPECT images (Figure 2) compared to PET images (Figure 1) to improve the visibility of areas of abnormality.

**Figure 1:** Mapping from colors to values used for display of PET statistics (# Std. Dev.) in Database Comparison (cf. Figure 2).

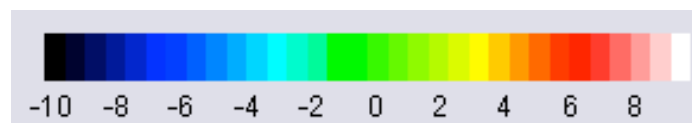


**Figure 2:** Mapping from colors to values used for display of SPECT statistics (# Std. Dev.) in Database Comparison (cf. Figure 1).



### Example: FDG-PET

Taking as an example an FDG-PET scan of a patient with suspected dementia (Figure 3), an area of interest is indicated by the position of the crosshair in the parietal lobe, where reduced tracer uptake was observed during the visual read of the images. Using the color table and range of values shown in Figure 1, statistics images such as those shown in Figure 4 are obtained, where the corresponding region shows as an area of negative values. The statistics here help to support a clinically relevant finding of reduced tracer uptake in the right parietal lobe due to a combination of atrophy and hypometabolism.

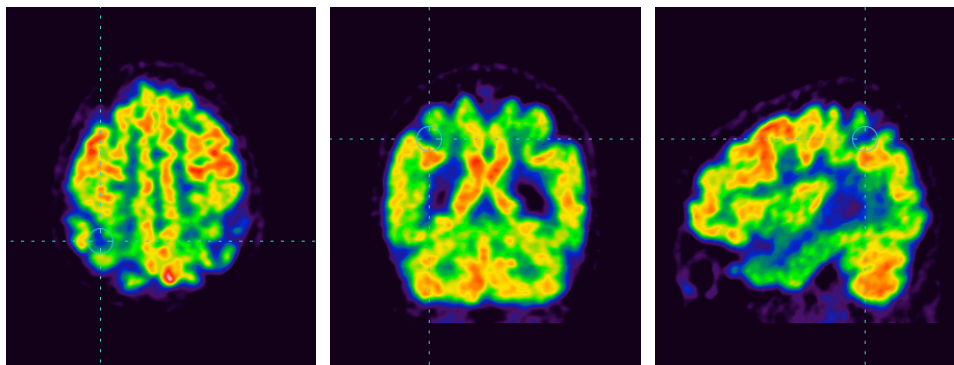


**Figure 3:** Axial, coronal, and sagittal slices through an FDG-PET image; the slices and cross-hair position used correlate with those shown in Figure 4.

Image courtesy of St. Claraspital, Basel, Switzerland.

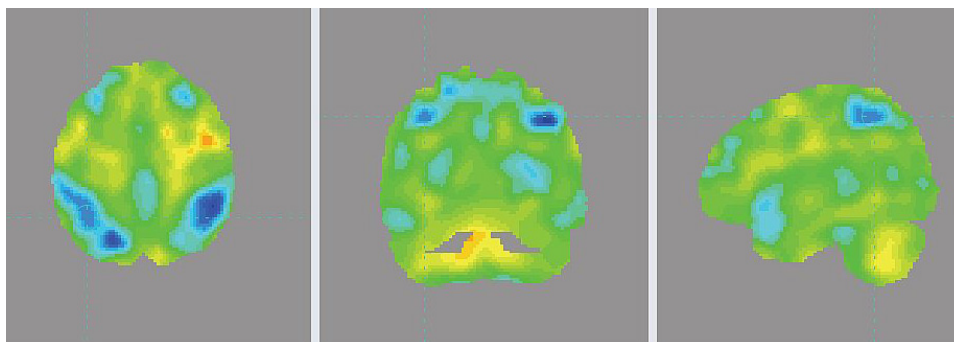


**Figure 4:** Axial, coronal, and sagittal slices through a statistics image for an FDG-PET image; note the negative statistics values (blue) around the crosshair.

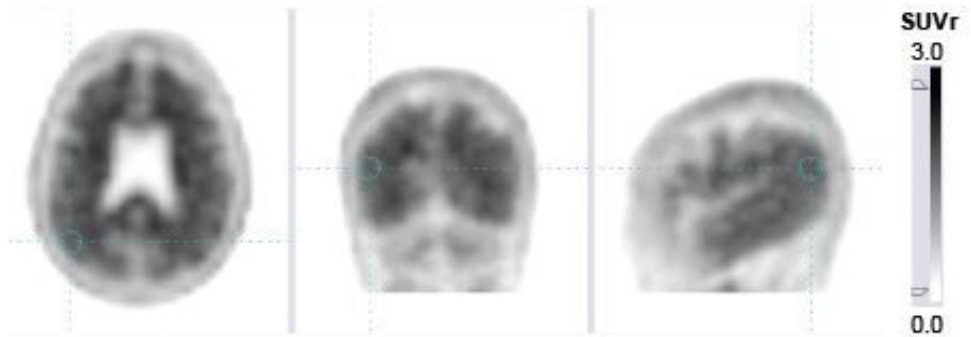
Image courtesy of Siemens Healthineers. Note that statistical images are not intended to be used in lieu of a full read of the uptake data.

### Example: amyloid-PET

The key question to answer when reading amyloid PET images (e.g. florbetapir or florbetaben) is whether there is a local loss of contrast between uptake of the tracer in grey matter and uptake in white matter.<sup>2</sup> SUVR images derived from the florbetapir uptake for a patient with a scan read as positive (Figure 5) show increased grey matter uptake and hence apparent loss of contrast in the parietal and mesial frontal lobes; the corresponding area of the statistics images (Figure 6) show positive statistics, supporting the original visual finding.

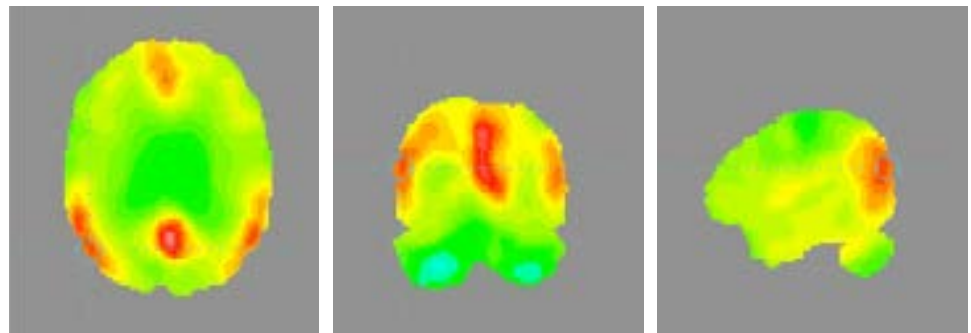
**Figure 5:** Axial, coronal, and sagittal slices showing SUVR values through an amyloid PET image; the slices and crosshair position used correlate with those shown in Figure 6. This case shows increased cortical SUVR nearly everywhere; white and grey matter cannot be delineated as in healthy subjects.

Image courtesy of Siemens Healthineers.



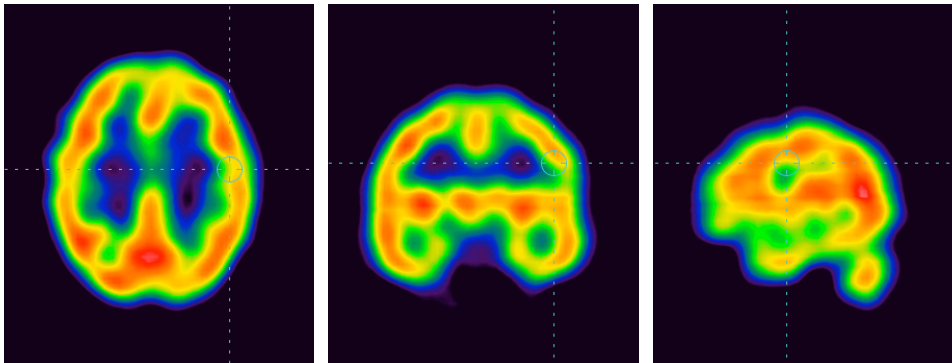
**Figure 6:** Axial, coronal, and sagittal slices through a statistics image for an amyloid PET image; note for instance the positive statistics values around the crosshair in the parietal lobe.

Image courtesy of Siemens Healthineers. Note that statistical images are not intended to be used in lieu of a full read of the uptake data.



### Example: ECD-SPECT

For comparison, uptake images of a clinically normal subject acquired with ECD-SPECT are shown in Figure 7. The corresponding statistics images (Figure 8) do not show areas of large positive or negative statistics, as expected for this healthy individual.



**Figure 7:** Axial, coronal, and sagittal slices through an ECD-SPECT image; the slices and crosshair position used correlate with those shown in Figure 8.

Images courtesy of Department of Nuclear Medicine, University of Erlangen, Germany.

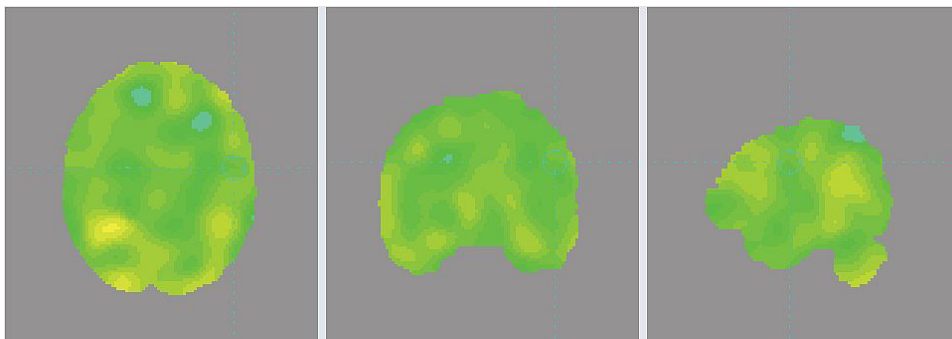


**Figure 8:** Axial, coronal, and sagittal slices through a statistics image for an ECD-SPECT image; note the lack of large positive or negative statistics.

Image courtesy of Siemens Healthineers. Note that statistical images are not intended to be used in lieu of a full read of the uptake data.

### Statistical significance

The statistics computed for the subject image provide a measure indicating how much the subject's uptake deviates from uptake at the corresponding position in the normal database population. A larger statistic (in terms of absolute value) indicates a larger deviation (which may be higher or lower) from the normal population. Deciding whether the statistic represents a significant difference from the normal population (e.g. a true finding), requires further calculations to determine how likely it is that the statistic was obtained by chance. These calculations are not performed in Database Comparison and users should refer to a text book on classical statistics<sup>3</sup> or brain image analysis<sup>4</sup> for correct implementation. The purpose of the calculations is summarized briefly below and a rule-of-thumb practical guide to interpretation of the statistics image is provided.

In general, deciding whether or not an individual statistical result is significant can be achieved by converting the statistic to a p-value. The p-value is the probability of obtaining the statistic by chance. A result is considered to be statistically significant when the p-value is below a predetermined significance level (typically 0.05 or 0.01). A larger statistic corresponds to a lower probability of obtaining that statistic by chance, e.g. a smaller p-value. The conversion of a statistic to a p-value involves comparing the statistic to the appropriate probability distribution for the number of degrees of freedom; note that for Database Comparison, the number of degrees of freedom is dependent on the number of cases in the database.

To assign statistical significance to the statistics image created by Database Comparison, two factors must be taken into account. The first is that there are many thousands of voxels in the image so many statistical values need to be compared to the statistical threshold corresponding to the predetermined significance level. This is, therefore, known as the multiple comparison problem. The second factor is that the data from any one voxel will tend to be similar to the data from nearby voxels, because the voxel values are spatially correlated as a result of image acquisition, reconstruction, physiological signals, and any spatial processing applied to the data such as registration and smoothing. The following describes corrections required to take account of these two factors:

- i) The Bonferroni correction<sup>3</sup> is a simple and conservative method to account for the multiple comparison problem. The p-value for an individual statistic is the probability of obtaining the statistic by chance. However, when there is an increase in the number of statistical values being assessed, there is also an increase in the likelihood of obtaining a statistic with a p-value below the predetermined significance level by chance. The Bonferroni Correction is therefore based on the idea that if  $n$  independent statistical values are assessed and the predetermined significance level for all statistics values is  $\alpha$ , then each statistic should be compared to a probability threshold of  $\alpha/n$ . This is a conservative correction that tends to underestimate the probability threshold because it assumes the voxels are independent, which is typically not the case.
- ii) Since the voxels are spatially correlated, the number of independent observations is, effectively, substantially less than the total number of voxels in the image. A more appropriate significance level can be found using the mathematics of Random Field Theory (RFT).<sup>5</sup> Using RFT, the first step is to estimate the spatial correlation or smoothness of the statistical image. This allows the total number of voxels in the image to be expressed as a number which is similar to the number of independent observations<sup>6</sup> and hence a correction for multiple comparisons based on RFT can be derived.



As a rule-of-thumb guide to interpretation of the statistics image in Database Comparison (for PET and SPECT), an individual statistic greater than 1.68 (in absolute value) approximately corresponds to a p-value less than 0.05 (note this assumes that either positive values only or negative values only are considered, e.g. this is a one-tailed test). However, after considering the problems of multiple comparisons and spatial correlation of voxels, findings with an individual statistic below approximately 4.6 for a database comprising 30 subjects and down to less than 4.2 for a database comprising 57 subjects, would typically not be considered as significant (this is based on an ad hoc estimate that the number of independent observations is 1,000 in a spatially processed PET image<sup>[a]</sup>). In general, the probability of a true finding increases with the size and magnitude of a potential lesion or region of abnormal uptake.

Due to the considerations outlined in this section, it is, therefore, critical that all findings in the statistics image are correlated with the original uptake image to determine diagnostic relevance.

### Region of interest-based statistics

As well as the voxel-based statistics discussed in the previous section, Database Comparison also calculates statistics based on three dimensional regions of interest (ROIs). To calculate ROI statistics, the population mean and standard deviation values for a particular ROI are computed by first calculating the mean value in that ROI for each of the normal subjects and then computing the mean and standard deviation of those mean values; the statistic can then be computed from those values and the mean uptake within the same ROI for the patient case. It is important to understand that the ROI statistics are not the average of the voxel-based statistics within the ROI; rather, they are computed by applying Equation 1 to the mean uptake value within the ROI.

Nevertheless, the validity of the result depends on the precision of the ROI definition. Especially in small ROIs, the accuracy of an individual ROI's position could be limited even when the overall volume registration to the template worked well. This is something that can happen due to individual anatomical variability, which cannot be compensated for completely by the registration algorithm; a visual check of the ROI position is, therefore, recommended. The averaging effect of region size (increasing the number of voxels with larger ROIs) typically leads to more stable results in large regions.

<sup>[a]</sup> Applying the Bonferroni correction to give an updated p-value  $<0.05/1000=0.00005$  requires the statistic greater than 4.6 (in the case of 56 degrees of freedom).

# Processing prior to analysis

Preparing a new subject image for analysis requires several tasks to be performed for the analysis to be robust:

1. selection of an appropriate database for comparison;
2. rigid registration to align any anatomical images loaded to the functional image being analyzed, to facilitate correlation of findings;
3. registration (affine and possibly non-linear), to align the subject images to the database;
4. smoothing of the functional image (for the purpose of processing only, not for display) to account for small differences in brain physiology and anatomy (e.g. gyri position);
5. intensity normalization, to eliminate global uptake differences between the functional image and the database.

Note that items (1), (2), and (3) are explicitly visible in the software, while items (4) and (5) are internal properties of the database selected and included here for completeness.

## Database selection

The first step when commencing analysis of a new subject study is to select an appropriate database for the statistics calculation. Database Comparison offers a number of different databases, but in general, the following items should be considered when making that choice:

- What modality and tracer were used for the image acquisition?
- What reconstruction algorithm (e.g. HD•PET, 3D-OSEM, FBP) was used to reconstruct the subject dataset? What scatter correction and post-reconstruction filters were used? For the best statistics, a protocol that matches the one used by the normal images within the database is highly desirable (for details, see the Database Comparison online help or Operator Manual).
- What type of attenuation correction (AC) was performed during reconstruction? The same type of AC (e.g. CT-based vs. Chang for SPECT images, or CT-based vs. SMART Neuro AC for PET images) should be used, otherwise systematic artifacts may appear in the statistics.
- Where multiple, otherwise equivalent databases with different normalization regions are offered, which one is most appropriate for the subject? As an example, a subject with abnormal uptake in the cerebellum should not be analyzed with a database that uses the cerebellum for intensity normalization.
- Where multiple, otherwise equivalent databases with different age-ranges are offered, which one is most appropriate for the age of the subject?
- Where multiple, otherwise equivalent databases with different degrees of smoothing are offered, which one is most appropriate for the required analysis?
- Where multiple, otherwise equivalent databases built with subjects of different genders or handedness are offered, which one is most appropriate for the subject?

In an ideal situation, a database would be selected that exactly matched the subject image in terms of the above parameters; however, in practice there is some tolerance in the parameters, especially when smoothing is used. Importantly, differences between the database parameters and subject image should be considered during analysis.

### Rigid registration of anatomical data

Database Comparison supports loading of a CT and/or MR image in addition to the functional image being analyzed, since such images can be useful when trying to interpret findings and explain artifacts in the statistics images. In order to support correlation of findings between all images, these anatomical images are aligned to the functional data using a rigid registration algorithm. This alignment is performed in all cases, even when the data was acquired on a hybrid scanner (e.g. PET/CT), since it is possible that a manual adjustment was made to the alignment of the images prior to AC of the PET image, a transformation that is not typically encoded in either dataset.

### Alignment of subject images to database

The key to performing a successful comparison to a database is the spatial normalization algorithm used to align the subject image to database standard geometry.<sup>7,8</sup> This algorithm needs to account for differences in anatomy between subjects, as well as coping with different patterns of uptake in the images due to disease, other pathologies, as well as functional variability.

Due to the variations in uptake with different tracers and modalities, Database Comparison contains several strategies for alignment to the database, with each database defining its own default strategy. The first step of all these registration strategies is to perform a linear affine registration to account for global position and scaling differences; for some databases, a non-linear (or deformable) registration algorithm is additionally employed to further reduce differences between the subject and the database, allowing for localized adjustments affecting only certain parts of the brain.

### Smoothing

Smoothing the subject dataset prior to image analysis is typically necessary due to differences in image resolution, scanners, reconstruction protocols, and anatomical variations that are not compensated for with registration (e.g. gyri position). Some databases are provided with multiple levels of smoothing, although the majority are smoothed using an isotropic Gaussian filter of size 12 mm full-width at half-maximum.<sup>9-12</sup> Details of the smoothing used for individual databases can be found in the “Individual database details” section.

## Intensity normalization

For PET images, standardized uptake values (SUVs) can potentially provide a degree of normalization of raw intensity values (although see<sup>13,14</sup> for some limitations); however, such standardized values are not typically available for SPECT images and comparison to a database requires a more robust approach to ensure that the variation between the subject image and the database solely reflects pathology. The standard technique from the literature<sup>10,15-18</sup> is to identify a region of the brain where tracer uptake is not expected to be affected by disease and to scale the intensities in the brain by a statistic (e.g. mean) derived from voxels within that ROI. Database Comparison uses this approach; in some cases providing databases built with the same data, but using different regions for the intensity normalization to enable analysis of subjects with pathology in one of the normalization ROIs.

Note that in order to reduce the number of outliers, intensity normalization is performed after the smoothing is applied to the image.

In order to further improve robustness of the estimate of the average activity within the ROI used for normalization (especially when using large regions of interest such as the whole brain), Database Comparison typically uses only a subset of the brightest voxels within the ROI when computing the mean—effectively computing a robust maximum; details of how this affects the individual databases can be found in the “Individual database details” section.

# Database construction

Construction of the normal databases provided by Database Comparison follows the same processing steps outlined in the section entitled “Processing Prior to Analysis.” A key aspect of the system is to ensure that exactly the same pipeline of operations is applied to each dataset when constructing the database as used for the subject data being analyzed. In this way, any systematic errors in that pipeline are reflected in the database statistics (for example, in increased standard deviation values) and, whilst these may reduce sensitivity in certain locations, they should improve overall robustness of the final statistics.

When building the databases provided with the system, all processing steps are performed using the automatic algorithms to ensure that no bias is introduced, for example, by using manual registration; this approach results in some otherwise acceptable normal subjects being excluded from the database. Before inclusion in the database, all subject images are clinically read to ensure that they are free from abnormalities and, in many cases, additional exclusion criteria is applied to ensure the best quality of normal data.

Note that full details of the acquisition protocols recommended for reconstructing images to compare against the databases are available in the Database Comparison online help or Operator Manual.

## Individual database details: FDG-PET

### ECAT HR+ databases for elderly subjects

Two databases (Table 1) are built from FBP reconstructions of ECAT HR+ scanner data. The healthy volunteers underwent genetic testing and were all APOE4 negative. Each healthy volunteer also completed a range of neuropsychological tests. Details of the patient selection and preparation can be found in reference 19.

Name	FDG1A	FDG1B
Acquisition	ECAT HR+	
Reconstruction	FBP with transmission AC, Hanning filter of 0.40 cycles per pixel	
Registration scheme	FDG affine + deformable	
Smoothing	12 mm FWHM	
Intensity normalization	Cerebellum (25% brightest voxels)	Whole brain (25% brightest voxels)
Number of subjects	30	
Age range	54-72	
Gender	Mixed	

**Table 1:** Data courtesy of Banner Health, Phoenix, AZ, USA.

### Biograph TruePoint databases for elderly subjects

Six databases are built from Biograph™ TruePoint scanner data, using 3D-OSEM and HD•PET reconstruction algorithms and using CT-based AC and SMART Neuro AC. Four of these databases (Table 3) use the whole brain for intensity normalization, whereas the remaining two databases (Table 2) use the cerebellum for intensity normalization. The healthy volunteers whose images are used in the database completed a range of neuropsychological tests and passed an MRI investigation.

**Table 2:** Data courtesy of St. Claraspital, Basel, Switzerland.

Name	FDG2A	FDG3A
Acquisition	Biograph TruePoint	
Reconstruction	3D-OSEM with CT-AC, 6 iterations, 21 subsets, 3 mm Gauss filter	HD•PET with CT-AC, 8 iterations, 21 subsets, 2 mm Gauss filter
Registration scheme	FDG affine + deformable	
Smoothing	12 mm FWHM	
Intensity normalization	Cerebellum (25% brightest voxels)	
Number of subjects	33	
Age range	46-79	
Gender	Mixed (22 female, 11 male)	

**Table 3:** Data courtesy of St. Claraspital, Basel, Switzerland.

Name	FDG2B	FDG2Bs	FDG3B	FDG3Bs
Acquisition	Biograph TruePoint			
Reconstruction	3D-OSEM with CT-AC, 6 iterations, 21 subsets, 3 mm Gauss filter	3D-OSEM with SMART Neuro AC, 6 iterations, 21 subsets, 3 mm Gauss filter	HD•PET with CT-AC, 8 iterations, 21 subsets, 2 mm Gauss filter	HD•PET with SMART Neuro AC, 8 iterations, 21 subsets, 2 mm Gauss filter
Registration scheme	FDG affine + deformable			
Smoothing	12 mm FWHM			
Intensity normalization	Whole brain (25% brightest voxels)			
Number of subjects	33			
Age range	46-79			
Gender	Mixed (22 female, 11 male)			

### Biograph mCT and Biograph TruePoint database for younger subjects

Two databases (Table 4) are built from 3D-OSEM reconstructions of a mixture of Biograph TruePoint and Biograph mCT™ scanner data with CT AC. The PET scans of these young, healthy volunteers were clinically read and diagnosed as normal.

Name	FDG4A	FDG4B
Acquisition	Biograph TruePoint and Biograph mCT	
Reconstruction	3D-OSEM with CT-AC: 17 cases with 6 iterations, 21 subsets, 3 mm Gauss filter; 20 cases with 4 iterations, 21 subsets, 3 mm Gauss filter	
Registration scheme	FDG affine <sup>[b]</sup> + deformable	
Smoothing	12 mm FWHM	
Intensity normalization	Cerebellum (25% brightest voxels)	Whole brain (25% brightest voxels)
Number of subjects	37	
Age range	19-44	
Gender	Mixed (10 female, 28 male)	

**Table 4:** Data courtesy of Rigshospitalet, Copenhagen, Denmark; Oslo University Hospital, Oslo, Norway.

### Individual database details: florbetapir-PET

The normal florbetapir database (Table 5) is derived from florbetapir-PET scans of subjects who were required to have a Mini-Mental State Examination (MMSE) score of 29 or greater and to be cognitively normal based on psychometric testing. The florbetapir-PET normal database further complements SUV ratio analysis, which is also available for this type of study.

Name	Florbetapir-2A
Acquisition and reconstruction	Mixed, but reconstructed to a common standard <sup>20</sup>
Registration scheme	Deformable
Smoothing	12 mm FWHM
Intensity normalization	Cerebellum Central (all voxels)
Number of subjects	57
Age range	50-93
Gender	Mixed (26 female, 31 male)

**Table 5:** Data courtesy of Avid Radiopharmaceuticals Inc., a wholly-owned subsidiary of Eli Lilly and Company.

<sup>[b]</sup> Note that the fixed dataset used to drive the registration algorithm is not the same as the one used for the elderly FDG-PET databases, and hence, (slightly) different alignments may be observed when analyzing a case with both young and elderly FDG databases.

## Individual database details: florbetaben-PET

The normal florbetaben database (Table 6) is derived from florbetaben-PET scans of subjects who were required to have a Mini-Mental State Examination (MMSE) score of 28 or greater and Clinical Dementia Rating (CDR=0). The florbetaben-PET normal database further complements SUV ratio analysis, which is also available for this type of study.

Name	Florbetaben-1A
Acquisition and reconstruction	Mixed, but reconstructed to a common standard <sup>21</sup>
Registration scheme	Deformable
Smoothing	12 mm FWHM
Intensity normalization	Cerebellum Central (all voxels)
Number of subjects	54
Age range	55-85
Gender	Mixed (32 female, 22 male)

**Table 6:** Data courtesy of Piramal Imaging, Warwick, United Kingdom

## Individual database details: ECD-SPECT

Seven databases (Tables 7, 8, and 9) for ECD-SPECT are provided in Database Comparison, with properties as set out below. Each scan included in the ECD databases was clinically read and checked to be free of any abnormalities. Anatomical imaging (CT and/or MR) was without relevant findings. Patient history was used to exclude inappropriate cases.

Name	ECD1A	ECD1B
Acquisition	MultiSPECT3 with LEUHR <sup>[c]</sup> collimators	
Reconstruction	FBP with Chang AC, Butterworth filter 5th order (cut-off frequency of 0.3)	
Registration scheme	SPECT affine	
Smoothing	12 mm FWHM	
Intensity normalization	Brainstem (25% brightest voxels)	Whole brain (25% brightest voxels)
Number of subjects	30	
Age range	50+	
Gender	Mixed	

**Table 7:** Data courtesy of Erlangen University Hospital (Nuklearmedizinische Klinik mit Poliklinik der Friedrich-Alexander-Universität Erlangen-Nürnberg), Erlangen, Germany.

<sup>[c]</sup> LEUHR: low energy ultra-high resolution



Name	ECD2A	ECD2B
Acquisition	MultiSPECT3 with LEUHR collimators	
Reconstruction	FBP with Chang AC, Butterworth filter 5th order (cut-off frequency of 0.3)	
Registration scheme	SPECT affine	
Smoothing	12 mm FWHM	
Intensity normalization	Brainstem (25% brightest voxels)	Whole brain (25% brightest voxels)
Number of subjects	36	
Age range	35-65	
Gender	Mixed	

**Table 8:** Data courtesy of Erlangen University Hospital (Nuklearmedizinische Klinik mit Poliklinik der Friedrich-Alexander-Universität Erlangen-Nürnberg), Erlangen, Germany.

Name	ECD3A	ECD3B	ECD3C
Acquisition	MultiSPECT3 with LEUHR collimators		
Reconstruction	FBP with Chang AC, Butterworth filter 5th order (cut-off frequency of 0.3)		
Registration scheme	SPECT affine		
Smoothing	12 mm FWHM		None
Intensity normalization	Brainstem (25% brightest voxels)	Whole brain (25% brightest voxels)	
Number of subjects	30		
Age range	16-49		
Gender	Mixed		

**Table 9:** Data courtesy of Erlangen University Hospital (Nuklearmedizinische Klinik mit Poliklinik der Friedrich-Alexander-Universität Erlangen-Nürnberg), Erlangen, Germany.

## Individual database details: HMPAO-SPECT

HMPAO SPECT scans were performed on healthy volunteers as a part of a follow-up on asymptomatic controls in a dementia study. All asymptomatic controls were given the same comprehensive examination, including medical and psychiatric examination, blood and CSF collection, EEG, CT, rCBF, orthostatic test, and cognitive tests. Additionally, a three-year cognitive follow-up and EEG was performed. Inclusion criteria were intact cognitive function and activities of daily living during the follow-up period. Exclusion criteria were physical or mental disease affecting cognitive status and fulfillment of the criteria for any dementia disorder or mild cognitive impairment. HMPAO scans that were visually abnormal according clinical assessment were excluded as well.

Four databases are provided for HMPAO-SPECT analysis:

Name	HMP1A	HMP1B	HMP2A	HMP2B
Acquisition	Symbia™ SPECT/CT			
Reconstruction	Flash3D with CT-AC, 8 iterations, 8 subsets, 7 mm Gauss filter		FBP with Chang AC, Butterworth filter 5th order (cut-off frequency of 0.325)	
Registration scheme	SPECT affine			
Smoothing	12 mm FWHM			
Intensity normalization	Brainstem (25% brightest voxels)	Whole brain (25% brightest voxels)	Brainstem (25% brightest voxels)	Whole brain (25% brightest voxels)
Number of subjects	20			
Age range	64-86			
Gender	Mixed			

**Table 10:** Data courtesy of Lund University Hospital, Lund, Sweden.

## User-created databases

Database Comparison supports user creation of new databases, which can then be used for analysis in exactly the same way as the standard system databases. As discussed at the start of the “Database Construction” section, to obtain the best statistics it is important to control the processing applied to datasets used in the construction of the database carefully; Database Comparison, therefore, applies some constraints on the registration performed when aligning a candidate subject to the standard template space.

In particular, when creating a new database, a choice of modality and tracer is made, and this choice (combined with the modality of the data) determines the registration strategy that will be used to align new subjects to the new database. Database Comparison requires that potential additions to the database have been registered using the default automatic registration scheme as the final step (although manual repositioning is allowed, if required, to provide a better starting alignment). In general, if a tracer that is used in a system database is chosen, then the corresponding registration scheme for that database will be used; if a tracer previously unknown to Database Comparison is entered, then CT registration (as used for florbetapir-PET) will be used. The consequence of this constraint is that only scans with an accompanying CT image can be included in databases for previously unknown tracers.

Finally, because Database Comparison does not offer the possibility of executing all registration schemes for all tracers, in order to ensure that the required registration scheme is performed on the dataset being added to the database, a database for the same tracer should be selected on start-up. If no such database exists (because the new database is for a previously unknown tracer), then one of the “Template” databases available in the “Other” radiopharmaceutical section should be selected.

When considering adding a new subject to a database that is under construction, it is advisable to compare the scan to an existing database (where possible) to check that there are no unexpected abnormalities in the image. If a system database exists already, then that can be used, or once a number of scans have been added to the new database, the statistics produced by comparison can be useful in determining whether a case is suitable for inclusion in the database or not.

It is recommended to include at least 20 subjects (ideally more) in a database before using it clinically.<sup>22</sup> The number of cases should be sufficient to cover variability in anatomy as well as functional uptake; databases with fewer subjects will result in a warning being given by the system.

## Spatial normalization for database alignment

In order to obtain reliable statistics when comparing to a database, accurate alignment between the subject being analyzed and the database is essential. Of course, different subjects have brains of slightly different sizes and shapes, so rigid registration (consisting of translation and rotation only) is insufficient. Scaling must also be considered,<sup>23</sup> and in Database Comparison, a minimum of full affine registration consisting of translation, rotation, scaling, and shearing is used as in Reference 9.

All databases provided by Database Comparison are defined in the standard Montreal Neurological Institute (MNI) space,<sup>24</sup> as used by other packages such as SPM.<sup>25</sup>

The registration strategies for alignment to the database in the software consist of two key components: a dataset in the desired geometry of the database, used as the fixed or source volume, and a registration algorithm that optimizes the transformation between that fixed dataset and the subject dataset. It is the combination of the details of these two components that provide the reliable alignment necessary for database comparison.

### FDG-PET

For FDG-PET images, once the initial affine alignment has been performed, an additional deformable (non-linear) registration is executed. This additional step helps refine the alignment, especially around the edges of the brain.

### Amyloid PET

Registration of amyloid PET images poses a particular challenge due to the dramatic difference in uptake patterns between amyloid-positive and amyloid-negative PET scans. A new PET-based deformable (non-linear) registration technique was developed to align an input amyloid PET image to a corresponding database. This algorithm is initialized by an affine alignment.

## ECD- and HMPAO-SPECT

For SPECT images that are typically lower resolution than PET images, Database Comparison uses affine registration, reducing the overall time taken to align the subject to the database.

## Manual adjustment

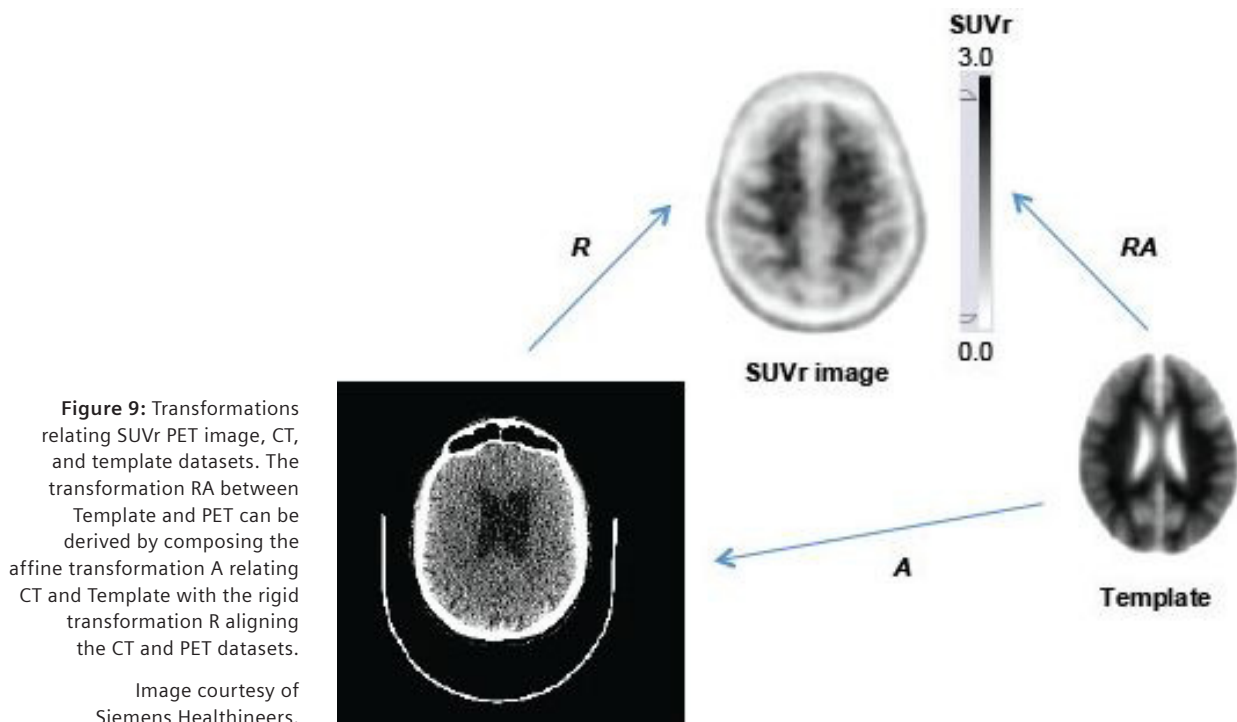
The alignment computed automatically by Database Comparison can be overridden if required, for example, in the unusual case of the automatic registration performing sub-optimally. However, due to the complexity of interactions with the three-dimensional dataset, only manual affine registration is available when aligning the subject to the database, even if the automatic algorithm had computed a non-linear transformation.

When the automatic algorithm fails, it is often due to poor initial alignment rather than a persistent failing of the algorithm itself. In this case, performing a quick manual affine adjustment to the dataset can provide a good enough starting point that the automatic algorithm can then succeed; Database Comparison provides tools for re-launching the automatic registration algorithm based on the current alignment of the datasets.

## CT-based affine alignment

For some complex cases, the automatic deformable registration to a database may fail due to poor initial alignment. If a CT dataset is loaded alongside the functional image, the user could perform a CT-based affine registration algorithm to initialize and re-launch the automatic deformable registration.

In addition, if a CT data is available, then the user can override the alignment computed automatically by Database Comparison with a CT-based affine alignment. In this case, an affine registration that aligns the CT image to the database is first performed and then the resulting transformation is composed with the rigid alignment between the functional and CT images (Figure 9) to obtain the final affine transformation aligning the input functional image to the database.



Ideally the same processing should be used both when constructing the database and when analyzing a subject. However, because the statistics computed for the normal subjects in a database will implicitly include information from systematic errors in the automatic registration algorithm, if a different alignment strategy (e.g. manual adjustment or CT-based) is used to align the subject to the database, it is possible that artifacts will be produced in the statistics image. It is, therefore, recommended that the final registration performed before analysis is always the standard automatic algorithm for that database, unless the failure of alignment continues after improving the initial position.

## Summary displays

In addition to the standard orthogonal slices, Database Comparison also supports display of a stereotactic surface projection (SSP).<sup>16</sup> The SSP view provides a visual impression of the entire cortex of the brain at once, using a tableau of eight images, as shown in Figure 10. The use of a three-dimensional lighting effect can help explain the eight images being shown more easily, as seen in Figure 12. Six of the views (right and left lateral, anterior, posterior, superior, and inferior) are computed as if observing the brain from the corresponding direction; the final two views are computed by slicing vertically down the brain mid-line and presenting data on the two exposed “faces.”

Two different algorithms are used for computing the SSP images, depending on the tracer: for FDG-PET, HMPAO-SPECT, and ECD-SPECT, an algorithm based on the uptake image, which is similar to that popularized by Minoshima,<sup>16</sup> is used; for amyloid-PET (florbetapir and florbetaben) and other “new tracer” databases, a modified SSP method, based on an atlas, is used to compute the statistics and uptake SSP views.

### Standard stereotactic surface projection

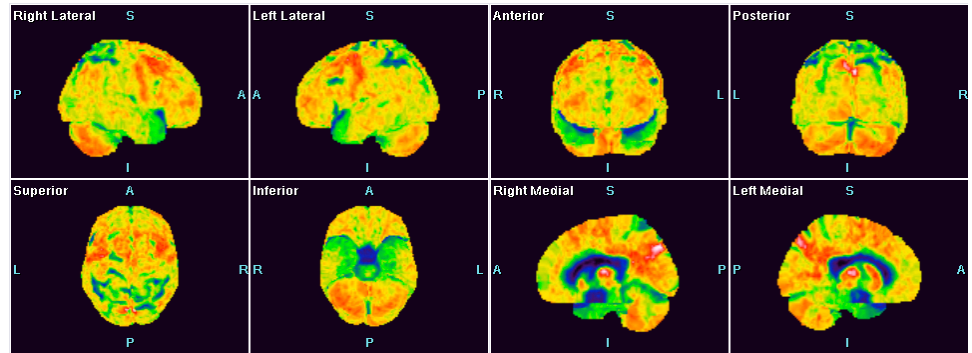
Fundamentally, the computation of each of the eight images within the SSP view is based on the idea of taking normal vectors to the brain surface and projecting these into the cortex of the brain to a depth of 13 mm.<sup>16</sup> The voxel intensities (of the uptake image) along each of these projections are then considered, and the maximum intensity value recorded. These values are then rendered such that the image they create corresponds to the view of the brain from the particular direction required (see, e.g. Figure 10). This image is referred to as the uptake SSP.

Once the uptake SSP is created, the statistics SSP can be computed by taking the voxel locations of the maximum intensity voxels found when computing the uptake SSP, and looking up the corresponding intensity from the statistics image before rendering in the same way, thus ensuring that the uptake and statistics SSP views always show consistent data.

One key difference between the statistics SSP views presented by Database Comparison and those of Minoshima<sup>16</sup> is that Database Comparison computes the voxel-wise statistics for the entire three-dimensional brain volume and then renders these as an SSP view as described above. Minoshima, by contrast, computes the database data in SSP space and hence the statistics SSPs displayed by Minoshima are the direct comparison of the uptake SSP views to the database.

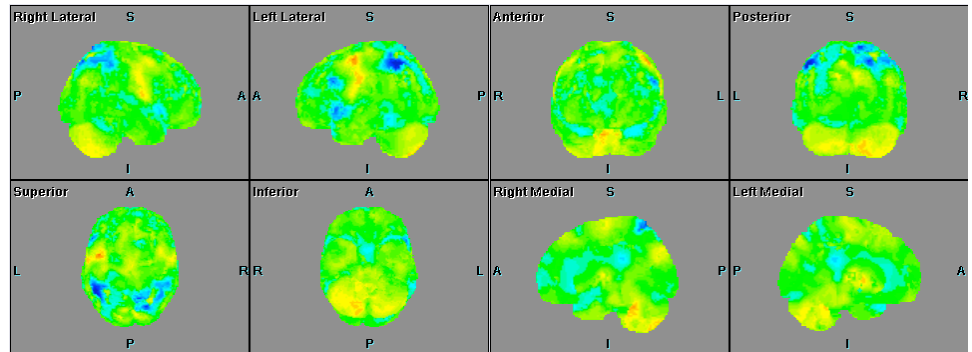
**Figure 10:** Stereotactic surface projection of uptake image for a FDG-PET case; cf. Figure 3. Note area of reduced uptake in the region of the parietal lobe.

Image courtesy of Siemens Healthineers. Note that statistical images are not intended to be used in lieu of a full read of the uptake data.



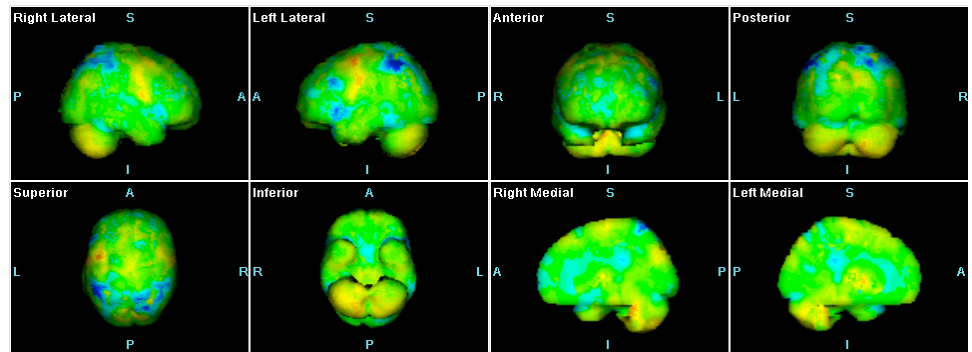
**Figure 11:** Stereotactic surface projection of statistics image for a FDG-PET case. The area of reduced uptake in the region of the parietal lobe visible in Figure 10 appears as an area of negative statistics (blue).

Image courtesy of Siemens Healthineers. Note that statistical images are not intended to be used in lieu of a full read of the uptake data.



**Figure 12:** Stereotactic surface projection statistics images with three-dimensional lighting effect; cf. Figure 11.

Image courtesy of Siemens Healthineers. Note that statistical images are not intended to be used in lieu of a full read of the uptake data.



## Modified stereotactic surface projection

The algorithm described in the previous section contains a fundamental assumption: that the maximum intensity encountered along the normal vector projection will be due to clinically relevant tracer uptake. For FDG-PET, HMPAO-SPECT, and ECD-SPECT, this assumption is valid, because the tracer accumulates only in the grey matter of the cortex and, if a normal vector projection strays into white matter, only low uptake will be encountered.

However, for amyloid PET tracers such as florbetapir and florbetaben, this assumption is invalid (Figure 13): high white matter uptake is expected, and thus the crude assumption that a global depth of 13 mm is suitable for all subjects is wrong: artifacts will appear in the statistics SSP whenever grey matter is closer than 13 mm to the apparent brain surface computed by registration.

In order to support an SSP-equivalent display for such tracers, an alternative approach is taken to the calculation: rather than first computing the uptake SSP and then deriving the statistics SSP from that, a fixed set of 3D voxel coordinates is generated in MNI space for each of the eight projection directions (see Figure 10). These coordinates are used to sample projection values from the spatially normalized uptake and statistics images and display the corresponding SSP views. These eight sets of voxel coordinates are calculated based on the spatial distribution of grey matter in a population of brain images of three diagnostic groups (normal volunteers, mild cognitive impairment, and Alzheimer's disease) normalized to MNI space. With this method, projected SSP views for a given amyloid PET image will contain values that are sampled from the cortex after it is spatially normalized to MNI space. This is justified because, for such tracers, the white matter uptake is usually consistent whatever the disease state, and hence, the statistics for white matter uptake will show fairly "normal" low absolute values. Thus, the modified SSP algorithm ensures that when looking for the maximum statistics value along a normal projection vector, only relevant values are identified.

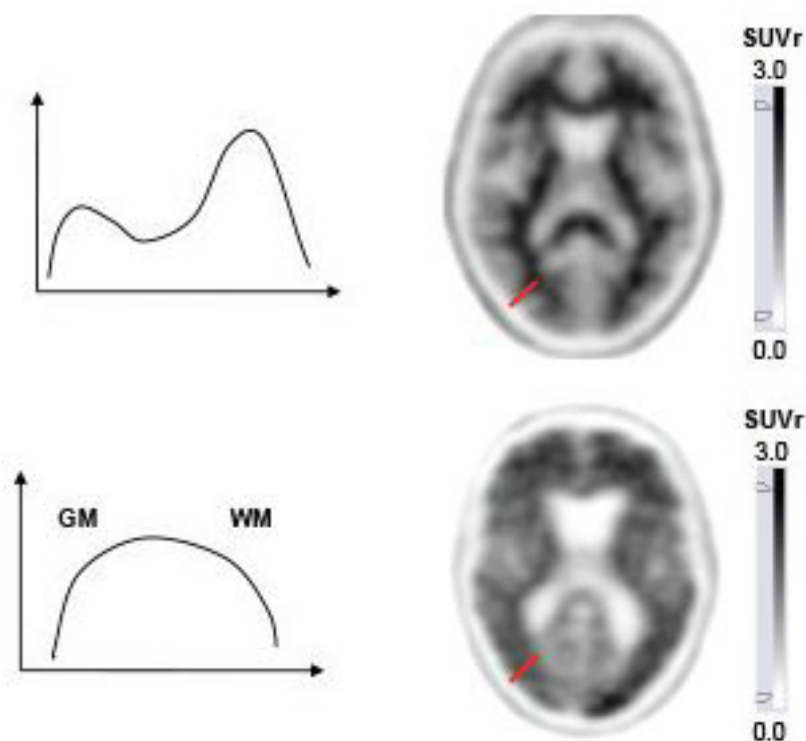


**Figure 13:** Schematic line profiles (along the red lines marked) through SUVr amyloid PET images for a negative scan (top) and a positive scan (bottom). Note that in positive images, the separation of grey matter (GM) and white matter (WM) is ambiguous.

Image courtesy of Siemens Healthineers.

# Potential artifacts

Due to the variation of subjects, disease patterns, image acquisition, and processing within Database Comparison itself, it must always be borne in mind that findings in the statistics image could be artifacts unrelated to disease. Not all anatomical and functional variability can be captured in the model of variability represented in the statistics map. In the sections below, some of the commonly seen artifacts are shown, along with tips for how to identify them.

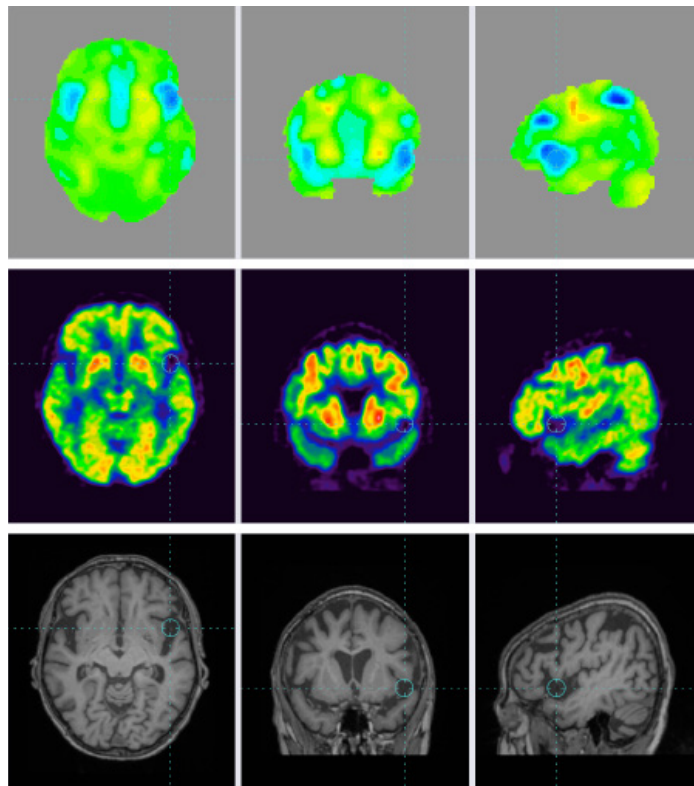
## Abnormal subject brain structure

In some subjects, abnormal physical structure of the brain (either inherent, or caused by previous unrelated pathology or surgery) is present and the lack of tracer uptake in these areas can manifest as lower than expected statistics.

Figure 14 (top row) shows the statistics images for an FDG-PET image, where an unexpected area of low statistics is indicated by the crosshair. Looking at the corresponding position in the uptake image (Figure 14, middle row), it is clear that there is a genuine lack of FDG uptake in that area, and correlation with the MR image (Figure 14, bottom row) gives confirmation that the cause is perisylvian atrophy. In this case, there is no problem with the system and, now that the cause of the finding is known, the analysis can continue.

**Figure 14:** Statistics, uptake and MR images for an FDG-PET study; note the unusually low statistics (blue) in the neighbourhood of the crosshair (top row), corresponding low uptake in the FDG-PET images (middle row), and perisylvian atrophy visible in the MR image in the region of the crosshair (bottom row), the cause of the 'missing' FDG uptake.

Data courtesy of St. Claraspital, Basel, Switzerland. Note that statistical images are not intended to be used in lieu of a full read of the uptake data.





## Registration artifacts

Registration artifacts often manifest themselves at the edges of the brain, where the automatic alignment has failed to fully compensate for the shape of the subject data. A relatively subtle example is given in Figure 15, which shows the SUVr and statistics images for a florbetapir amyloid PET scan and a registration artifact under the crosshair.

From the statistics image alone, it cannot be determined whether the unexpectedly high statistics are caused by a registration problem. The subject MR image shows clearly the origin of the elevated statistics (Figure 16): the crosshair position is bound throughout Database Comparison, so, by placing the crosshair at the edge of the brain in the statistics image (Figure 15), it is clear from the same location in Figure 16 that the registration algorithm has not correctly identified the edge of the brain in the florbetapir amyloid PET and, hence, MR images. The apparently high statistics are caused by the white matter florbetapir uptake being pulled too close to the brain boundary by the affine registration and being compared to grey matter statistics in the database.

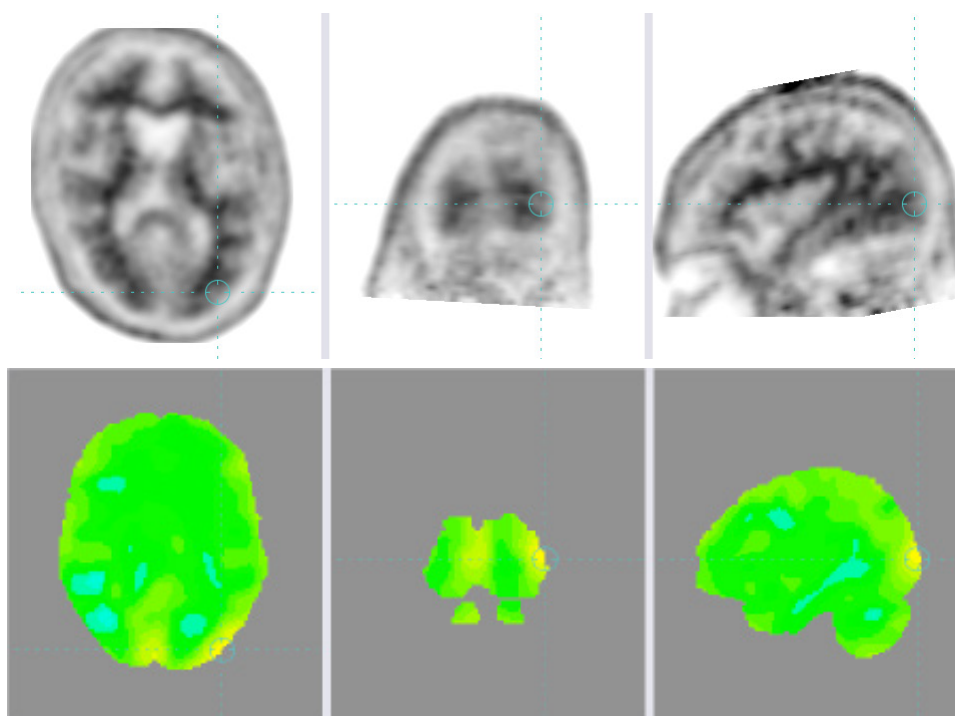


**Figure 15:** Manifestation of a registration artifact in the statistics image for the SUVr of an amyloid PET dataset (top); note the elevated statistics values (bottom) around the crosshair.

Images courtesy of Siemens Healthineers. Note that statistical images are not intended to be used in lieu of a full read of the uptake data.

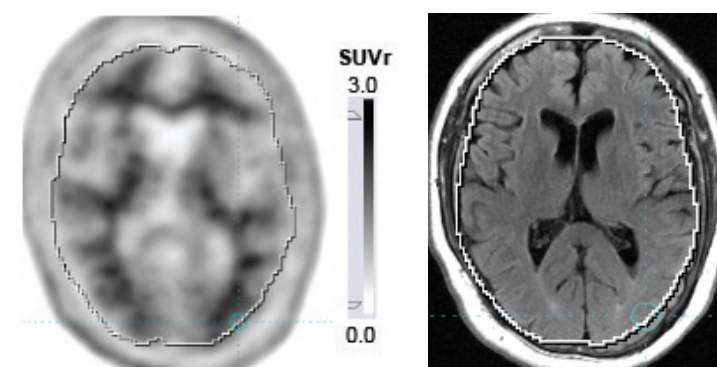


**Figure 16:** Example of SUVr amyloid PET image (left) and MR image (right) with template brain boundary overlaid with the crosshair in the same location as in Figure 15; note how the crosshair is clearly well within the subject's brain boundary in this image, but at the edge of the template brain as determined by the system.

Image courtesy of Siemens Healthineers.

The solution to this problem is to manually adjust the affine transformation aligning the amyloid PET image to the database, which is likely best achieved in this case by using the MR image, where the brain boundary is much more clearly identified (assuming that the alignment between the MR and PET datasets is accurate).

### Intensity normalization issues

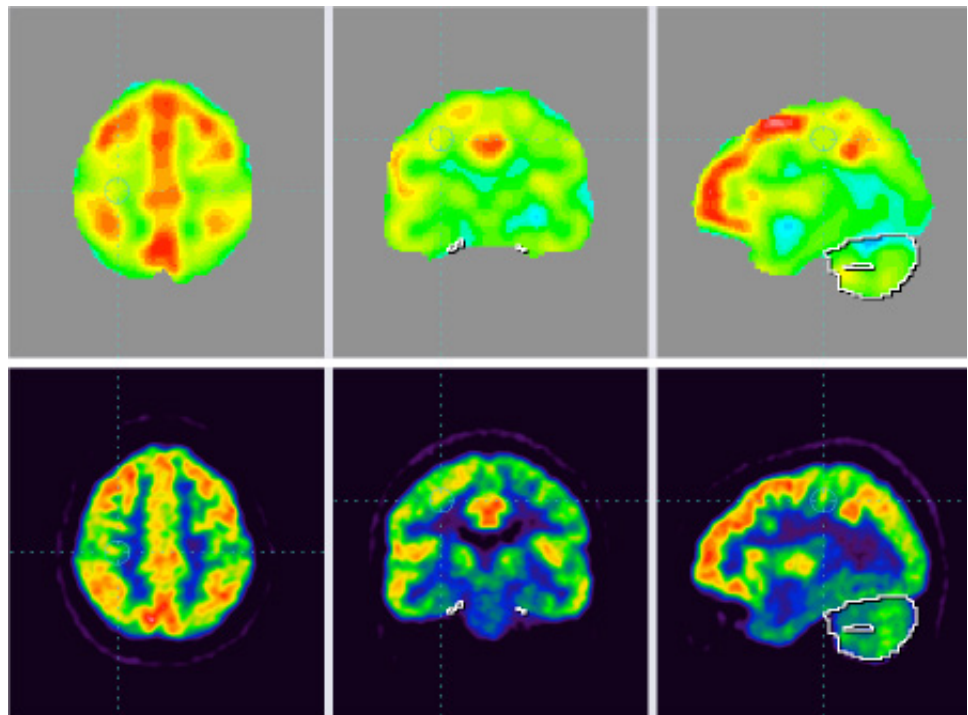
Normalizing the intensities of the subject image to eliminate global differences in tracer uptake is essential to obtaining an accurate comparison to the database. However, the region of interest approach used by Database Comparison can exhibit artifacts if the subject has unusual uptake in the normalization ROI relative to the rest of the brain.

Figure 17 (top row) shows statistics for an FDG-PET image where there is an unexpected pattern of high values in several areas of the brain. Crucially, these statistics were computed by comparing to a database with the cerebellum used for intensity normalization. The choice of this database assumes that the cerebellum is normal and can be used as reference.

Comparing to the corresponding uptake images in Figure 17 (bottom), it can be seen that the ratio of the uptake between the cerebellum and the cortex is unusual: the cerebellum exhibits lower uptake than would typically be expected. Given this discrepancy, the statistics images in this case must be treated with extreme caution.

**Figure 17:** Statistics (top) and uptake (bottom) images for an FDG-PET dataset compared to a database using the cerebellum for intensity normalization. Note the elevated values (red) in the frontal and parietal lobes and the more normal (green) values in the cerebellum.

Top: Images courtesy of Siemens Healthineers. Bottom: Images derived from data courtesy of St. Claraspital, Basel, Switzerland. Note that statistical images are not intended to be used in lieu of a full read of the uptake data.



### Abnormal area of uptake

Subjects sometimes exhibit unusually high (in comparison to normal database) tracer uptake in parts of the brain without underlying disease. Reasons could include activation effects (e.g. visual or auditory stimulation during the “resting” period post-injection but prior to the acquisition), and also statistical noise due to the multitude of evaluated voxels. Figure 18 (top) shows statistics corresponding to an FDG image of a subject where there is an area of unexpectedly high statistics indicated by the crosshair.

Figure 18 (bottom) shows the corresponding uptake images, where it is clear that there is some preserved activity in that region of the brain and, therefore, the finding in the statistics is real, even if clinically irrelevant.

### Atrophy artifact for florbetapir-PET images

Due to atrophy of the cortical grey matter, the separation of the two hemispheres of the brain can differ between subjects. The lack of uptake of amyloid PET tracers in either the grey matter of normal subjects or in areas of the image that correspond to gaps left by the atrophy means that both the mean and standard deviation of voxels near the midline are small. However, in the particular case of an amyloid PET study where the brain has a relatively low degree of atrophy (in comparison to the average population) with uptake of the amyloid PET tracer in the cortical grey matter (see Figure 19-top for a florbetapir case), the statistics can exhibit a very high value near the midline, as shown by the crosshair position in Figure 19 (bottom).

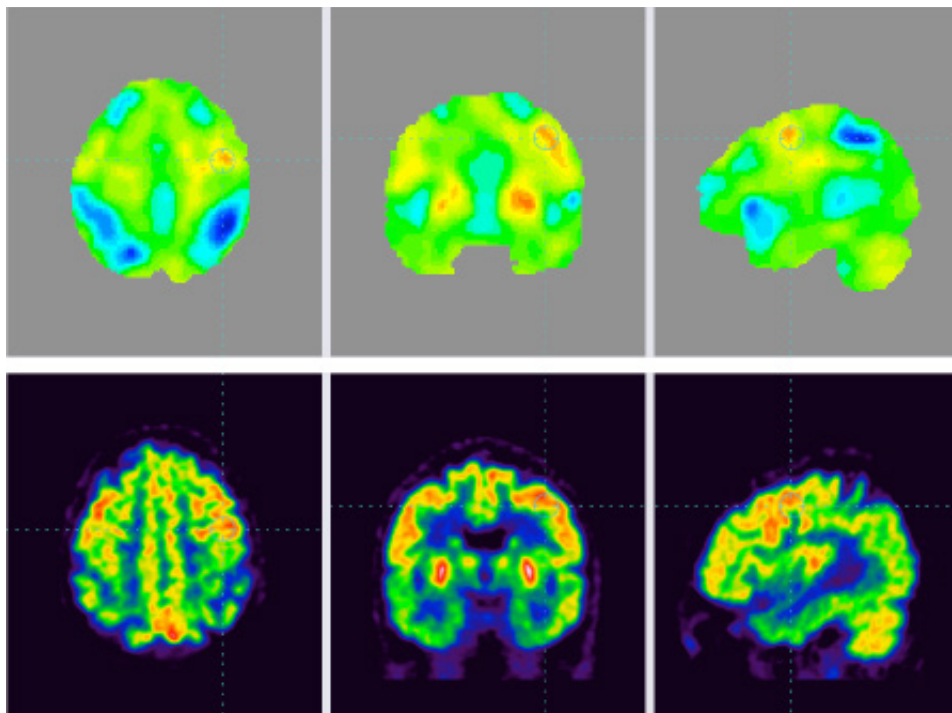
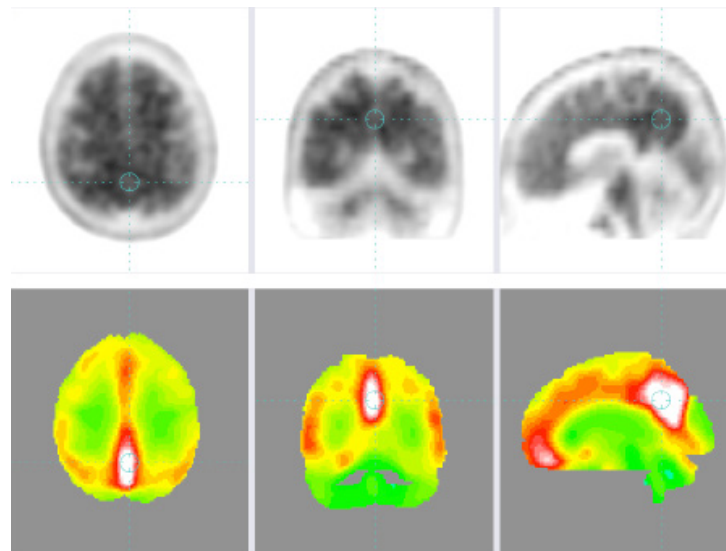


Figure 18: Statistics (top) and uptake (bottom) images for an FDG-PET dataset; note the high statistics (orange) visible around the crosshair (top) and the preserved activity in the central/precentral region (bottom).

Top: Images courtesy of Siemens Healthineers. Bottom: Images derived from data courtesy of St. Claraspital, Basel, Switzerland. Note that statistical images are not intended to be used in lieu of a full read of the uptake data.

## Marrow uptake artifact for amyloid PET images

Some small proportion of subjects exhibit high bone marrow uptake during florbetapir amyloid PET image acquisition (see Figure 20-top for a florbetapir case). While Database Comparison only computes statistics for voxels within the brain, the use of smoothing during the analysis means that uptake from voxels that are outside the brain (e.g. in the bone marrow or scalp) can influence the statistics. This is not a problem if subjects with similar uptake are well represented in the normal population used to create the database, but where an uptake pattern occurs only infrequently in the population, it can substantially affect the statistics image.



**Figure 19:** SUVr (top) and statistics (bottom) for an amyloid PET image of a subject with a relatively low degree of atrophy, where an unexpectedly high value is observed near the midline of the brain.

Images courtesy of Siemens Healthineers. Note that statistical images are not intended to be used in lieu of a full read of uptake data.

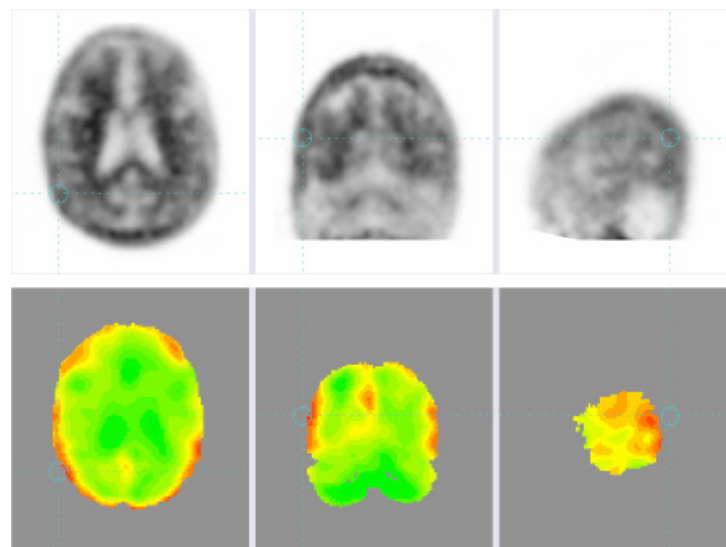


**Figure 20:** SUVr (top) and statistics (bottom) for an amyloid PET image of a subject with unusually high SUVr in the bone marrow. Note the rim of high statistics values around the edge of the brain (bottom).

Images courtesy of Siemens Healthineers. Note that statistical images are not intended to be used in lieu of a full read of uptake data.

# Conclusion

Comparison of a subject image to a database built from a normal population can provide useful additional information when performing a clinical read. Database Comparison is a software system that supports such analysis for a variety of tracers, providing robust computational algorithms to automate much of the necessary preparation of images.

For users with access to their own source of normal data, Database Comparison offers the possibility of creating new normal databases, for example, tailored for specific populations or even for new tracers.

However, there are some important areas that should be appreciated when performing an analysis: appropriate selection of a database for comparison; awareness of the possibility of non-clinically relevant artifacts in the statistics image; and understanding of how to interpret the significance of statistics presented by the system.

# About the authors

**Rachid Fahmi, PhD**, received a MSc and a Doctorate degree in Applied Mathematics from University of Metz, France and then completed a PhD in Electrical and Computer Engineering at the University of Louisville, KY in 2008. He has worked in the field of medical imaging since 2003 at the University of Louisville and at Case Western Reserve University, OH. He's been with the Research and Clinical Applications team of Siemens Molecular Imaging as a staff scientist since the summer of 2015, leading scientific development of software solutions for molecular imaging applications in Neurology.

**Günther Platsch, MD**, studied medicine at the University of Erlangen-Nuremberg from 1982 and passed the final exams 1988. From 1988 to 2004 he worked as an assistant physician, later as a senior physician at the department of Nuclear Medicine of that University. He received a Doctorate degree in Medicine in 1991 (Dr. med.) and became a board certified Nuclear Medicine Physician in 1992. In 2004 Günther Platsch joined Siemens AG as a clinical scientist in Siemens Molecular Imaging, since 2011 as a Senior Key Expert. In this position he provides medical input for clinical application development as well as in SPECT and PET development.

# Acknowledgment

We would like to thank Dr. Thomas Wright for his pioneering contribution to the development of MI Neurology applications and for authoring an earlier version of this paper.

# References

- <sup>1</sup> **Bohnen NI, Djang DS, Herholz K, et al.** Effectiveness and safety of <sup>18</sup>F-FDG PET in the evaluation of dementia: a review of the recent literature *Journal of Nuclear Medicine* 2012;53(1):59-71
- <sup>2</sup> **The Amyvid Reader Training Program.** <https://amyvid.myregistrationp.com/amyvid/index.do>
- <sup>3</sup> **Bland M.** An introduction to medical statistics, Third Edition, Oxford University Press, 2000.
- <sup>4</sup> **Friston KJ, Ashburner JT, Kiebel SJ, Nichols TE, Penny WD.** eds. Statistical Parametric Mapping: The Analysis of Functional Brain Images. London, U.K. Academic Press; 2007
- <sup>5</sup> **Siegmund DO, Worsley KJ.** Testing for a Signal with Unknown Location and Scale in a Stationary Gaussian Random Field. *Annals of Statistics*, 23:608-39, 1994
- <sup>6</sup> **Worsley KJ, Evans AC, Marrett S, Neelin P.** A three-dimensional statistical analysis for CBF activation studies in the human brain. *Journal of Cerebral Blood Flow and Metabolism*, Volume 12, pp.900-918, 1992
- <sup>7</sup> **Fox PT, Perlmutter JS, Raichle ME.** A stereotactic method of anatomical localization for positron emission tomography. *J Comput Assist Tomogr.* 1985;9:141–15
- <sup>8</sup> **Friston KJ, Passingham RE, Nutt JG, Heather JD, Sawle GV, Frackowiak RS.** Localisation in PET images: direct fitting of the intercommissural (AC-PC) line. *J Cereb Blood Flow Metab.* 1989;9:690–69
- <sup>9</sup> **Herholz K, Salmon E, Perani D, et al.** Discrimination between Alzheimer Dementia and Controls by Automated Analysis of Multicenter FDG PET, *NeuroImage* 17, 302-316 (2002)
- <sup>10</sup> **Ishii K, Willoch F, Minoshima S, et al.** Statistical Brain Mapping of <sup>18</sup>F-FDG PET in Alzheimer's Disease: Validation of Anatomic Standardization for Atrophied Brains, *Journal of Nuclear Medicine* Vol. 42 No. 4 548-557, 2001
- <sup>11</sup> **Matsuda H, Kitayama N, Ohnishi T, et al.** Longitudinal Evaluation of Both Morphologic and Functional Changes in the Same Individuals with Alzheimer's Disease *J. Nucl. Med.* 2002 43: 304-311
- <sup>12</sup> **Mosconi L, Pupi A, De Cristofaro MTR, Fayyaz M, Sorbi S, Herholz K.** Functional Interactions of the Entorhinal Cortex: An <sup>18</sup>F-FDG PET Study on Normal Aging and Alzheimer's Disease *Journal of Nuclear Medicine* Vol. 45 No. 3 382-392, 2004
- <sup>13</sup> **Huang SC.** Anatomy of SUV (Standardized Uptake Value). *Nuclear Medicine & Biology* 2000; 27: 643-646



- <sup>14</sup> **JW Keyes Jr.** SUV: standard uptake or silly useless value? *J. Nucl. Med.* 1995 36: 1836-1839
- <sup>15</sup> **Minoshima S, Frey KA, Foster NL, Kuhl DE.** Preserved pontine glucose metabolism in Alzheimer disease: a reference region for functional brain image (PET) analysis. *J Comput Assist Tomogr.* 1995 Jul-Aug;19(4):541-7
- <sup>16</sup> **Minoshima S, Frey KA, Koeppe RA, Foster NL, Kuhl DE.** A diagnostic approach in Alzheimer's disease using three-dimensional stereotactic surface projections of fluorine-18-FDG PET *J. Nucl. Med.* 1995 36: 1238-1248
- <sup>17</sup> **Bartenstein P, Minoshima S, Hirsch C, et al.** Quantitative assessment of cerebral blood flow in patients with Alzheimer's disease by SPECT *J. Nucl. Med.* 1997 38: 1095-1101
- <sup>18</sup> **Ishii K, Sasaki M, Kitagaki H, et al.** Reduction of cerebellar glucose metabolism in advanced Alzheimer's disease *J. Nucl. Med.* 38: 925-928,1997
- <sup>19</sup> **Reiman EM, Caselli RJ, Yun LS, et al.** Preclinical evidence of Alzheimer's disease in persons homozygous for the epsilon 4 allele for apolipoprotein E. *New England Journal of Medicine* 334(12):752-8, 1996
- <sup>20</sup> **Fleisher AS, Chen K, Liu X, et al.** Using positron emission tomography and Florbetapir F 18 to image cortical amyloid in patients with mild cognitive impairment or dementia due to Alzheimer disease. *Archive of Neurology.* 2011
- <sup>21</sup> **Barthel H, Gertz HJ, Dresel S, et al.** Cerebral amyloid-PET with florbetaben (<sup>18</sup>F) in patients with Alzheimer's disease and healthy controls: a multicentre phase 2 diagnostic study. *Lancet Neurol.* 2011;10(5):424–35
- <sup>22</sup> **Chen WP, Samuraki M, Yanase D, et al.** Effect of sample size for normal database on diagnostic performance of brain FDG PET for the detection of Alzheimer's disease using automated image analysis *Nuclear Medicine Communications* 2008, 29;3:270-276
- <sup>23</sup> **Bradley KM, O'Sullivan VT, Soper NDW, et al.** Cerebral perfusion SPET correlated with Braak pathological stage in Alzheimer's disease *Brain*, Aug 2002; 125: 1772-1781
- <sup>24</sup> **MNI:** <https://www.mcgill.ca/neuro/>
- <sup>25</sup> **SPM99 and SPM2:** Wellcome Centre for Human Neuroimaging, Statistical Parametric Mapping software: <https://www.fil.ion.ucl.ac.uk/spm/software/spm12/>

**Legal information:** On account of certain regional limitations of sales rights and service availability, we cannot guarantee that all products included in this publication are available through the Siemens Healthineers sales organization worldwide. Availability and packaging may vary by country and is subject to change without prior notice.

The information in this document contains general technical descriptions of specifications and options as well as standard and optional features, which do not always have to be present in individual cases. Please contact your local Siemens Healthineers sales representative for the most current information.

Note: Any technical data contained in this document may vary within defined tolerances. Original images always lose a certain amount of detail when reproduced. All images © 2021 Siemens Healthcare GmbH. All rights reserved.

“Siemens Healthineers” is considered a brand name. Its use is not intended to represent the legal entity to which this product is registered. Please contact your local Siemens Healthineers organization for further details.

---

**Siemens Healthineers Headquarters**

Siemens Healthcare GmbH  
Henkestr. 127  
91052 Erlangen, Germany  
Phone: +49 9131 84-0  
siemens-healthineers.com

**Published by**

Siemens Healthineers USA, Inc.  
Molecular Imaging  
2501 North Barrington Road  
Hoffman Estates, IL 60192 USA  
Telephone: +1 847 304 7700  
siemens-healthineers.com/mi